Association of a Dynamin-like Protein with the Golgi Apparatus in Mammalian Cells

John R. Henley* and Mark A. McNiven*‡§

Departments of *Molecular Neuroscience and ‡Biochemistry and Molecular Biology, and §Center for Basic Research in Digestive Diseases, Mayo Clinic and Foundation, Rochester, Minnesota 55905

Abstract. Dynamins are a family of 100-kD GTPases comprised of at least three distinct gene products and multiple alternatively spliced variants. Homologies with the *shibire* gene product in *Drosophila melanogaster* and with Vps1p and Dnm1p in *Saccharomyces cerevisiae* suggest that dynamins play an important role in vesicular transport. Morphological studies have localized brain dynamin to coated pits and tubular invaginations at the plasma membrane, where it is believed to facilitate the formation of endocytic vesicles. Because similar membrane-budding events occur at the Golgi apparatus and multiple dynamin isoforms exist, we have studied the distribution of dynamins in mammalian cells. To this end, we generated and characterized peptide-specific antibodies directed against conserved regions of the dynamin family. By immunoblot analysis, these antibodies reacted specifically with a 100-kD protein in fibroblasts that sedimented with membranes and microtubules in vitro in a manner similar to brain dynamin. By immunofluorescence microscopy, these antibodies strongly labeled the Golgi complex in cultured fibroblasts and melanocytes, as confirmed by double labeling with a Golgi-specific antibody. Furthermore, Western blot analysis showed significant enrichment of a 100-kD dynamin band in Golgi fractions isolated from the liver. To substantiate these findings, we used a specific antidynamin antibody to immunoisolate Golgi membranes from subcellular Golgi fractions, as determined by EM and immunoblot analysis. This study provides the first morphological and biochemical evidence that a dynamin-like protein associates with the Golgi apparatus in mammalian cells, and suggests that dynamin-related proteins may have multiple cytoplasmic distributions. The potential contributions of dynamin to the secretory and endocytic pathways are discussed.

DYNAMIN is a 100-kD GTP-binding protein that was originally isolated from the bovine brain because of its ability to cross-link and bundle microtubules in vitro in a nucleotide-dependent manner (Shpetner and Vallee, 1989). The GTPase activity of dynamin is stimulated by microtubules (Maeda et al., 1992; Shpetner and Vallee, 1992; Tuma et al., 1993), phospholipids (Tuma et al., 1993), phosphorylation (Robinson et al., 1993), and certain Src homology 3 domain–containing proteins (Gout et al., 1993; Herskovits et al., 1993*b*; Scaife et al., 1994). While its precise function is presently undefined, substantial evidence has implicated dynamin at an early stage in endocytosis. Dynamin is believed to be the mammalian homologue of the *shibire* gene product in *Drosophila melanogaster* (Chen et al., 1991; van der Bliek and Meyerowitz, 1991), in which a temperature-sensitive mutation renders these flies paralyzed because of an inability to recycle synaptic vesicles at nerve terminals (e.g., Poodry and Edgar, 1979; Kosaka and Ikeda, 1983*a*; Costello and Salkoff, 1986; Koenig and Ikeda, 1989). Ultrastructural studies of different cell types from mutant *shibire* flies show an accumulation of membrane invaginations and a depletion of subplasmalemmal vesicles at the cell surface, consistent with a perturbation in endocytosis (Kosaka and Ikeda, 1983*b*; Costello and Salkoff, 1986; Kim and Wu, 1987; Kessell et al., 1989; Koenig and Ikeda, 1990). Furthermore, mutant forms of dynamin, when overexpressed in cultured cells, cause a marked reduction in receptor-mediated endocytosis (Herskovits et al., 1993*a*; van der Bliek et al., 1993; Damke et al., 1994, 1995). Finally, recent ultrastructural studies have confirmed the presence of dynamin on endocytic structures (Damke et al., 1994; Takei et al., 1995).

Several past studies suggested that dynamin was restricted to neural tissues (Scaife and Margolis, 1990; Nakata et al., 1991; Chen et al., 1992). This exclusive neuronal distribution was unexpected, since mutations in the *shibire* gene affect a number of different cell populations, including muscle (Buzin et al., 1978; Costello and Salkoff,

Please address all correspondence to Dr. Mark A. McNiven, Center for Basic Research in Digestive Diseases, Mayo Clinic and Foundation, 200 First Street SW, Rochester, MN 55905. Tel.: (507) 284-0683; Fax: (507) 284-0762.

1986), oocytes (Kessell et al., 1989), and garland cells (Kosaka and Ikeda, 1983*b*; Koenig and Ikeda, 1990). With the identification and cloning of two additional and distinct dynamin genes from epithelial tissues (Nakata et al., 1993; Cook et al., 1994; Sontag et al., 1994), it is now clear that dynamin isoforms are expressed in all cells. Conventional brain dynamin, dynamin I (Dyn1)[1], is indeed neuronal-specific (Nakata et al., 1991, 1993; Cook et al., 1994; Sontag et al., 1994); a second dynamin gene product, dynamin II (Dyn2), is ubiquitously expressed (Cook et al., 1994; Sontag et al., 1994); and a third, dynamin III, is restricted to testis (Nakata et al., 1993; reviewed in Robinson et al., 1994). It is also believed that multiple variants of the dynamin isoforms arise through alternative splicing (Sontag et al., 1994). A number of distinct proteins also share significant homology with the dynamin family at the amino-terminal domain. Of particular interest is the yeast vacuolar protein sorting protein, Vps1p, which is involved in protein sorting at the Golgi apparatus (Rothman et al., 1990; Vater et al., 1992; Wilsbach and Payne, 1993), and the recently identified Dnm1p, which is involved in endosomal protein trafficking in yeast (Gammie et al., 1995).

Although dynamin associates with microtubules in vitro, this has not been observed in vivo. Rather, immunocytochemical studies on the distribution of dynamin in PC12 cells (Scaife and Margolis, 1990) and intact neurons (Noda et al., 1993; Gass et al., 1995) reveal diffuse and punctate staining patterns that spread throughout cell bodies, neurites, and growth cones. A similar distribution is observed in transfected cells overexpressing Dyn1 (Herskovits et al., 1993*a*). Western blot analysis of subcellular fractions from the brain shows dynamin immunoreactivity in both membrane and cytosolic fractions. It is unclear whether dynamin associates with synaptic vesicles (Noda et al., 1993; Tuma et al., 1993) or an unidentified membrane compartment (Scaife and Margolis, 1990) in these preparations. More recently, dynamin has been localized to clathrin-coated pits at the plasma membrane in cultured cells (Damke et al., 1994), and to the necks of membrane invaginations and clathrin-coated pits in an isolated synaptosomal preparation (Takei et al., 1995). It is expected that the multiple dynamin isoforms and related proteins will have different distributions and functions that are not yet defined in mammalian cells. We have therefore constructed a library of five affinity-purified pAbs directed against three distinct regions of rat brain Dyn1 that are highly conserved within the dynamin family of proteins. Using morphological and biochemical methods, we examined the intracellular localization of dynamin in primary cultures of human cells of two different embryonic origins: fibroblasts (mesenchymal) and melanocytes (neural crest). By immunoprecipitation and Western blot analysis, these polyclonal antibodies (pAbs) specifically recognized purified rat brain dynamin, as well as dynamin from crude extracts of rat brain and cultured human fibroblasts. Indirect immunofluorescence microscopy of cultured cells showed that these antibodies consistently labeled a perinuclear membrane network that localized with a Golgi-specific antibody, but not with fluorescently labeled endocytic compartments. Interestingly, fibroblasts that were immunolabeled with a pAb to Vps1p also revealed a reticular Golgi association identical to that seen with the multiple antidynamin antibodies. Consistent with these morphological observations, Western blot analysis of subcellular organelle fractions isolated from rat liver showed a significant enrichment of a 100-kD dynamin protein in Golgi-enriched fractions as compared to a total membrane fraction. Furthermore, we demonstrate that a specific antidynamin antibody immunoisolated Golgi membranes from two separate subcellular Golgi fractions, as determined by EM and Western blot analysis. These biochemical and morphological observations provide the first evidence that a dynamin-like protein is associated with the Golgi apparatus in mammalian cells and may be involved in vesicular trafficking events of the secretory pathway.

1. *Abbreviations used in this paper*: CM, crude membrane fraction; D-PBS, Dulbecco's PBS; Dyn1, dynamin I; Dyn2, dynamin II; pAB, polyclonal antibody.

Materials and Methods

Materials

Tissues used for this study were harvested from 150–250 g male Sprague Dawley rats (Harlan, Madison, WI). Taxol was a gift from the National Cancer Institute (Bethesda, MD). Other reagents were from Aldrich Chemical Company, Inc. (Milwaukee, WI), Bio-Rad Laboratories (Hercules, CA), Calbiochem Corp. (La Jolla, CA), Electron Microscopy Sciences (Fort Washington, PA), Pharmacia Fine Chemicals (Uppsala, Sweden), or Sigma Chemical Co. (St. Louis, MO), unless specified otherwise. A pAb to rab 6 was purchased from Santa Cruz Biotechnology, Inc. (Santa Cruz, CA), and an mAb against β-COP was obtained from Sigma Chemical Co. Secondary antibodies were FITC- or TRITC-conjugated goat anti-rabbit and goat anti-mouse (Kirkegaard & Perry Laboratories, Gaithersburg, MD) for immunocytochemical staining; alkaline phosphatase- or HRP-conjugated goat anti-rabbit and goat anti-mouse (Biosource International, Camarillo, CA) were used for Western blot analysis. The following antibodies were obtained as gifts: the Golgi-specific mAb 10E6 (Dr. W. Brown, Cornell University, Ithaca, NY), a pAb to the catalytic domain of rat liver Golgi α-mannosidase II (Dr. M. Gist Farquhar, University of California, San Diego, CA), a rabbit anti-rab 6 (Dr. B. Goud, Institut Pasteur, Paris, France), mAb 3DI against RER-associated ribophorin II (Dr. D. Meyer, University of California, Los Angeles), and pAbs and mAbs to Vps1p (Dr. T. Stevens, University of Oregon, Eugene). Partially purified brain dynamin was a gift from Dr. G. Waters (Princeton University, Princeton, NJ).

Cells and Culture Conditions

Primary cultures of human foreskin melanocytes and fibroblasts were provided by the laboratory of Dr. M. Pittelkow (Mayo Clinic, Rochester, MN). Cells were grown at 37°C with 5% CO_2 in a humid environment using standard tissue culture procedures. Melanocytes were cultured in MCDB 153 media supplemented with 0.1 mM ethanolamine, 0.1 mM phosphorylethanolamine, and 0.5 μM hydrocortisone (Pittelkow and Shipley, 1989), while fibroblasts were cultured in MEM-α medium with L-glutamine, ribonucleosides, and deoxyribonucleosides (GIBCO BRL, Grand Island, NY) containing 10% FBS. Cells were grown in Falcon petri dishes (Fisher Scientific, Pittsburgh, PA) and on 12-mm round cover glasses for protein extraction and immunocytochemistry, respectively.

Production and Affinity Purification of pAbs

Peptides against the deduced amino acid sequence of rat brain Dyn1 (Obar et al., 1990) were synthesized and conjugated to keyhole limpet hemocyanin by the Mayo Protein Core Facility at the Mayo Clinic. These peptides were suspended in PBS and Freund's adjuvant, injected into New Zealand white rabbits, and the antisera were collected after subsequent boost injections. The peptide sequences (single-letter amino acid notation) and corresponding antibody names are LTLVDLPGMTKV (amino acids 132–143; MC12), IAVVGGQSAGKSSVLE (amino acids 34–48; MC13 and MC14), ARDVLENKLLPLRRGYIGVVNRSQKD (amino acids 216–

241; MC62 and MC63), and KEKASETEENGSDSF (amino acids 633–647; Dyn 1). The crude antisera were affinity purified using an agarose column conjugated with the appropriate HPLC-purified synthetic peptide and a low pH elution buffer, according to the manufacturer's directions (Pierce Chemical Co., Rockford, IL). The purified antibodies were dialyzed molecular weight cut-off [MWCO] (12,000–14,000) against Dulbecco's PBS (D-PBS; 8.1 mM Na_2HPO_4, 1.2 mM KH_2PO_4, pH 7.2, 138 mM NaCl, 2.7 mM KCl, 0.9 mM $CaCl_2$, 0.5 mM $MgCl_2$) containing 0.04% NaN_3, concentrated using polyethylene glycol, and in some cases, 2 μg/ml BSA was added. Affinity-purified antikinesin pAb MMR44 was prepared as described previously (Marks et al., 1994). A pAb to the rat polymeric IgA receptor was made to a peptide having the sequence QSSTIAAQVHDGPQEA, which represents amino acids 775–790 of the carboxyl terminus. All antibodies were stored at 4°C.

SDS-PAGE and Western Blotting

Protein concentrations were determined with bicinchoninic acid according to the manufacturer (Pierce), using BSA as a standard. Cellular proteins were separated by discontinuous SDS-PAGE under reducing conditions (Laemmli, 1970) on 5–10% and 5–12% polyacrylamide gradient gels or 7.5–9% linear gels, using a bisacrylamide/acrylamide ratio of 1:37.5. Protein bands were visualized with Coomassie brilliant blue or by silver staining (ICN Radiochemicals, Irvine, CA). Alternatively, proteins were electrophoretically transferred to polyvinyldifluoride membranes (Millipore, Bedford, MA) for Western blotting (Towbin et al., 1979). Membranes containing transferred proteins were blocked in TBS (20 mM Tris, pH 7.5, 150 mM NaCl) containing 5% BSA and 0.05% Tween 20 before incubation with primary antibodies. Immunoreactive bands were detected with an appropriate secondary antibody conjugated either to alkaline phosphatase or HRP. After each step, the membranes were washed with TBS containing 0.1–0.4% Tween 20. Membranes were developed with either bromochloroindoyl phosphate and nitro blue tetrazolium to visualize alkaline phosphatase or for enhanced chemiluminescence (Amersham Corp., Arlington Heights, IL) and were exposed to autoradiographic film (Eastman Kodak Co., Rochester, NY) to detect HRP. To quantitate the relative density of immunoreactive bands, exposed autoradiographic film was scanned with a densitometer (Shimadzu Scientific Instruments, Inc., Columbia, MD) or with a Umax Technologies, Inc. (Freemont, CA) scanner and analyzed with Adobe Photoshop (Adobe Photosystems, Inc., Mountain View, CA) and Image 1 (National Institutes of Health, Bethesda, MD) software. To estimate molecular weights, bands were referred to a high molecular weight standard mixture (SDS-6H; Sigma Chemical Co.) or to the following prestained standards: lysozyme, soybean trypsin inhibitor, carbonic anhydrase, ovalbumin, BSA, phosphorylase B, β-galactosidase, and myosin (Bio-Rad).

Purification of Dynamin and GTPase Assay

Dynamin was purified using a modification of the method by Scaife and Margolis (1990). Fresh rat brains were homogenized in a glass tissue grinder with a Teflon pestle (Wheaton Science Products, Millville, NJ) in 5 vol of buffer A (50 mM imidazole, pH 7.0, 100 mM KCl, 2 mM $MgCl_2$, 1 mM EGTA, 1 mM DTT, 0.5 mM PMSF, 10 μg/ml soybean trypsin inhibitor and leupeptin). The homogenate was centrifuged at 18,000 *g* for 30 min, and the supernatant was collected and recentrifuged at 110,000 *g* for 60 min. The resulting supernatant was passed over a 10-ml bed DEAE anion exchange column (DE-52; Whatman, Clifton, NJ), and the void volume was collected. This fraction was diluted 1:1 with buffer A without KCl and added to a 10-ml bed phosphocellulose cation exchange column (Whatman), washed with buffer B (10 mM MES, pH 6.8, 1 mM $MgSO_4$, 1 mM EGTA, 1 mM DTT, 0.5 mM PMSF) containing 100 mM NaCl, and eluted in the same buffer containing 250 mM NaCl (buffer C). The eluate was dialyzed (MWCO 12,000–14,000) against buffer B and applied to a GTP-agarose affinity column (Sigma Chemical Co.), washed with buffer B, and eluted with buffer C. This eluate was dialyzed (MWCO 12,000–14,000) against PEM/G buffer (5 mM Pipes, pH 7.0, 50 mM $C_5H_8NO_4Na$, 1 mM $MgSO_4$, 1 mM EGTA, 1 mM DTT), and will be referred to as purified brain dynamin. All procedures were carried out at 4°C, and aliquots were stored in 20% glycerol at −80°C.

Tubulin was purified from bovine brain as previously described (Gelfand et al., 1978) and assembled into microtubules at 37°C in buffer D (0.1 mM Pipes, pH 6.9, 1 mM $MgSO_4$) containing 0.1 mM GTP and 20 M taxol. Freshly purified rat brain dynamin was assayed for microtubule-activated GTPase activity with modifications to the method of Shpetner and Vallee (1992) using colorimetric measurement of phosphate release (Ames, 1966). The enzymatic activity of dynamin (1.5 g/ml) was determined at 37°C in PEM/G buffer either in the presence or absence of taxol-stabilized microtubules (0.3 mg/ml) with 0.75 mM GTP.

Protein Extraction and Immunoprecipitation

Cultured fibroblasts were harvested for biochemical analysis using standard procedures. Cells from 10–15 confluent petri dishes were rinsed two to three times with cold modified D-PBS without $CaCl_2$ or $MgCl_2$ (GIBCO BRL). Fibroblasts were scraped from the dishes with a cell lifter (Costar Corp., Cambridge, MA) in cold buffer A containing 0.5% Triton X-100 and then homogenized. Brain extracts were prepared by homogenizing one rat brain in 5 vol of buffer A with a glass tissue grinder (Wheaton Science Products). Homogenates were clarified by centrifuging at 8,500 *g* for 5 min. Alternatively, proteins were extracted by homogenizing in RIPA buffer (50 mM Tris, pH 8.1, 150 mM NaCl, 1 mM EDTA, 1% deoxycholate, 1% Triton X-100, 0.1% SDS, 1 mM PMSF, 100 g/ml soybean trypsin inhibitor, 10 g/ml leupeptin, 1 g/ml pepstatin) over a 20-min period and then clarified by centrifuging at 16,000 *g* for 5 min. All procedures were carried out at 4°C.

Immunoprecipitations were done using standard procedures at 4°C. Brains were homogenized and extracted in RIPA buffer as described above, while cultured fibroblasts were harvested after trypsinization and then sonicated in RIPA buffer (525 cm^2 confluent cells/ml). Homogenates were clarified by centrifuging at 210,000 *g* for 45 min, and in some cases, brain supernatants were precleared with protein A beads (Sepharose CL-4B; Pharmacia Biotech, Inc., Piscataway, NJ) to obtain cleared extracts. Anti-dynamin (MC12, MC13, and MC63) and antikinesin (MMR44) antibodies (3–30 μg) or normal rabbit serum (2.5–20 μl) were incubated with 1 μl (2–20 mg) of the protein extracts before adding preswollen protein A beads (3–20 mg). Incubation times were 2 h to overnight and were done on a nutator. Beads were collected by centrifuging at 7,000 *g* for 3 min and aspirating away the supernatant, and then washed extensively with RIPA buffer, wash buffer 1 (10 mM Tris, pH 7.4, 250 mM LiCl, 0.2% NP-40, 0.1% SDS), wash buffer 2 (20 mM Tris, pH 8.1, 150 mM NaCl, 1 mM $CaCl_2$, 1 mM $MgCl_2$, 0.2% NP-40), wash buffer 3 (10 mM Tris, pH 7.4), and 0.1% SDS before solubilizing the antibody/antigen complexes (immunoprecipitates) by boiling in 2× Laemmli sample buffer for 3 min.

Immunofluorescence and EM

For immunofluorescence microscopy, cells were grown on coverglasses for 2–7 d. Cells were rinsed with D-PBS at 37°C and fixed for 15–20 min with 2–3% formaldehyde in Pipes buffer (0.1 M Pipes, pH 6.95, 3 mM $MgSO_4$, 1 mM EGTA), which had been prewarmed to 37°C. After rinsing with D-PBS, cells were permeabilized with 0.05% Triton X-100 in D-PBS for 1–4 min, rinsed in D-PBS, and incubated in blocking buffer (5% normal goat serum and 5% glycerol in D-PBS) for 1 h at 37°C. Cells were incubated in primary antibodies (1–40 μg/ml) diluted in blocking buffer and rinsed repeatedly in D-PBS before incubating in the appropriate fluorescently labeled secondary antibody (1–5 μg/ml), also diluted in blocking buffer. Cells were then washed extensively with D-PBS, rinsed briefly with distilled water, and mounted on a glass slide in mounting reagent (SlowFade or SlowFade Light; Molecular Probes, Inc., Eugene, OR). For double-labeling experiments, cells were incubated simultaneously with both primary antibodies, rinsed with D-PBS, and incubated with two appropriate fluorescently labeled secondary antibodies. Cells were viewed with an Axiovert 35 epifluorescence microscope (Carl Zeiss, Inc., Thornwood, NY) equipped with a 50- or 100-W Mercury lamp using either a 63× or 100× objective lens (Zeiss Plan-Neofluar, NA 1.25 and 1.30, respectively). Images were recorded on Tmax p3200 or Ektachrome 400 film (Eastman Kodak Co.) with a 35-mm camera.

To label late endosomes and lysosomes, human fibroblasts were incubated with media containing 0.5 mg/ml lysine-fixable, FITC-conjugated dextran (3,000 mol wt; Molecular Probes) for 3.5 h at 37°C, rinsed with four changes of HBSS (Sigma Chemical Co.), and incubated for an additional 35 min at 37°C in media alone. Cells were then processed for indirect immunofluorescence microscopy as described above. In some cases, cells were photographed before immunocytochemical processing to compare the effect of processing on the dextran label.

For analysis by EM, suspended membrane (5–10 μl) and immunoisolated (0.2–1 mg beads) fractions were fixed in 2.5% glutaraldehyde (in 50 mM Na_2HPO_4/NaH_2PO_4, pH 7.4, 5 mM $MgCl_2$, 1 mM EDTA) for 0.5–1 h at 4°C. Membrane fractions were then embedded in 0.6% agarose and fixed an additional 1–6 h at 4°C in fresh 2.5% glutaraldehyde fixative. After rinsing in PBS, the fractions were postfixed in 2% osmium tetroxide

for 1.5 h, rinsed extensively in PBS, and stained overnight with 0.5% uranyl acetate. Fractions were then rinsed with two changes of PBS, dehydrated in a graded series of 50–100% ethanol, embedded in Quetol 651 (Ted Pella, Inc., Redding, CA), and sectioned with a diamond knife. Thin sections were poststained with lead citrate and viewed with a transmission electron microscope (JEOL 1200; JEOL USA, Peabody, MA) at 60 kV.

Subcellular Fractionation and Immunoisolation

For microtubule-binding experiments, fibroblasts and brains were homogenized as described above in PEM/G buffer containing 10 μg/ml soybean trypsin inhibitor and leupeptin. Homogenates (H) were centrifuged at 4°C for 30 min at 30,000 *g* and pellets collected as the heavy membrane fraction (P1). Supernatants were centrifuged at 170,000 *g* for 45 min and pellets collected as the microsomal fraction (P2), while supernatants were saved as the cytosolic fraction (S2). Microtubules were assembled from purified bovine brain tubulin as described above, stabilized with 20 μM taxol, and added to the S2 fraction. After a 30-min incubation at 37°C to allow dynamin to bind to the microtubules, this fraction was centrifuged at 170,000 *g* for 45 min at 20°C to yield a microtubule pellet (MtP) and supernatant (S3).

Enriched organelle fractions were isolated from rat liver according to the separate methods of Hamilton and co-workers (1991) and Howell and Palade (1982), as described in Marks et al. (1994). In addition, a modification of the method of Leelavathi et al. (1970) was used essentially as previously described (Fath et al., 1994). Briefly, a rat was anesthetized with pentobarbital (0.1 cc/100 g), and the liver was removed after perfusing with 40 ml of ice-cold PKM buffer (100 mM K_2HPO_4/KH_2PO_4, pH 6.65; 5 mM $MgCl_2$; 1 mM PMSF; 10 g/ml leupeptin, soybean trypsin inhibitor, and p-Toluenesulfonyl-L-arginine methyl ester; 5 μg/ml pepstatin; 50 μM DTT) containing 0.5 M sucrose. All the following steps were done at 4°C, and sucrose concentrations were maintained in PKM buffer with the aid of Milton Roy Co. (Rochester, NY) refractometers. In some experiments, Hepes buffer (25 mM Hepes-NaOH, pH 7.2; 5 mM $MgCl_2$; 1 mM EDTA; 1 mM PMSF; 10 g/ml leupeptin, soybean trypsin inhibitor, and p-Toluenesulfonyl-L-arginine methyl ester; 5 μg/ml pepstatin; 20 μM DTT) replaced the PKM buffer. The liver was finely minced and homogenized in 5 vol of 0.5 M sucrose with a polytron (Brinkmann Instruments, Inc., Westbury, NY), and the homogenate was centrifuged at 600 *g* for 10 min to obtain a postnuclear supernatant (S1). The postnuclear supernatant (10 ml) was layered over a 10-ml cushion of 1.3 M sucrose and was centrifuged at 105,000 *g* for 60 min. The supernatant was aspirated and the interface collected as the crude membrane fraction (CM). The CM fraction was adjusted to 1.1 M sucrose in 6.5 ml and layered onto a second discontinuous sucrose gradient containing 6.5-ml steps with sucrose concentrations as follows: 1.4, 1.3, 1.25, 1.1 (CM), and 0.5 M. This discontinuous sucrose gradient was centrifuged at 90,000 *g* for 1.5–2 h, and the flocculent material at the 0.5/1.1 M interface collected (3–5 ml) as the mixed Golgi fraction (G). This mixed Golgi fraction was adjusted to 0.5 M sucrose in a volume of 30 ml and was centrifuged at 10,000 *g* for 15 min. The pellet was gently resuspended in 0.5 M sucrose (0.25 ml) as the stacked Golgi fraction (Gs). The supernatant was centrifuged at 266,000 *g* for 30 min, and the pellet resuspended in 0.5 M sucrose (0.4 ml) as the Golgi vesicle fraction (Gv). A small fraction of the homogenate was centrifuged at 266,000 *g* for 45 min to obtain a total membrane pellet and a supernatant that was saved as the cytosolic fraction. Aliquots of all membrane fractions were diluted 5–10-fold in 0.5 M sucrose as a wash step, centrifuged at 266,000 *g* for 30 min, and pellets were resuspended in 2× RIPA buffer containing 1% SDS. Fractions were quick-frozen in liquid N_2 and stored at −80°C before subsequent analysis by Western blotting.

Immunoisolations were done as reviewed by Howell et al. (1989). Briefly, tosylated superparamagnetic beads (Dynabeads M-500 Subcellular; Dynal Inc., Lake Success, NY) were incubated overnight at room temperature on a rotator with a goat anti–rabbit linker antibody (Biodesign International, Kennebunkport, ME) at a concentration of 10 μg pAb/mg beads in borate buffer (100 mM H_3BO_3, pH 9.5). For this and all subsequent steps, beads were collected with a magnetic device (MPC, Dynal, Inc.). Beads were rinsed with incubation buffer (PBS containing 2 mM EDTA, 5% FBS) for 30 min, Tris buffer (50 mM Tris, pH 7.8, 100 mM NaCl, 0.1% Tween 20, 0.05% BSA) for 60 min, and incubation buffer for 30 min. The amount of linker antibody that bound to the beads was 5 μg/mg beads, as determined by OD_{280}. Coated Dynabeads (2–10 mg) were incubated for 12 h on a rotator with antidynamin pAb MC63 (10 μg pAb/mg beads) diluted in incubation buffer to a final volume of 1 ml. To obtain beads for control experiments, coated Dynabeads were incubated as above in incubation buffer alone. Beads (2–10 mg) were rinsed with two changes of incubation buffer and then incubated overnight at 4°C on a rotator with 0.15–0.25 mg of a Golgi membrane fraction (25–30 μg protein/mg beads) in 1 ml of incubation buffer. Golgi membrane fractions were either the Gs described above or a mixture of Golgi heavy and Golgi light fractions obtained using the procedure of Howell and Palade (1982), as described in Marks et al. (1994). Beads were then collected, rinsed with incubation buffer, and saved as the imunoisolated fractions. Supernatants that remained after separation from the immunoisolated fractions were centrifuged at 16,000 *g* for 10 min, and the pellets were resuspended in 0.25 M sucrose as the unbound fractions. Fractions were subsequently analyzed by standard EM and Western blotting techniques.

Results

pAbs Recognize Dynamin In Cell Homogenates

pAbs were generated against three different peptides representing regions of the amino-terminal domain of rat brain Dyn1 (Fig. 1) that are conserved among the dynamin family of proteins (Obar et al., 1990; Chen et al., 1991; van der Bliek and Meyerowitz, 1991; Nakata et al., 1993; Cook et al., 1994; Sontag et al., 1994). Two of these peptides spanned the first (MC13 and MC14) and second (MC12) regions of the dynamin tripartite GTP-binding motif (Obar et al., 1990), and they are conserved among the various dynamin-related proteins. A third peptide sequence (MC62 and MC63) was chosen based on its high degree of conservation within the dynamin family and lack of homology with related GTP-binding proteins. Crude rabbit antisera were collected and affinity purified, and the specificity of each antibody was determined by Western blot analysis. As shown in Fig. 2, each antidynamin antibody recognized a prominent protein in the brain and fibroblast extracts that migrated with purified brain dynamin. A similar profile was observed with pAbs MC14 and MC62 (data not

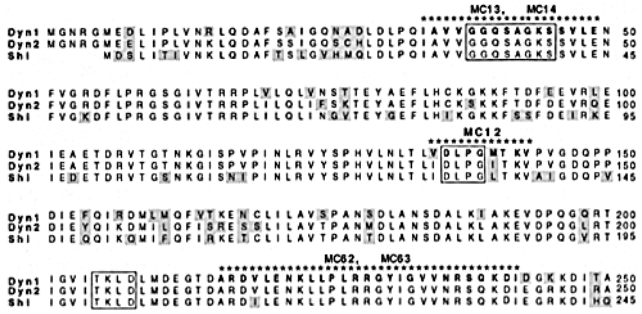

Figure 1. Selection of dynamin sequences for production of peptide antibodies. A comparison of the deduced amino-terminal amino acid sequences (single-letter amino acid notation) of the neuronal-specific Dyn1 (Obar et al., 1990), the ubiquitously expressed Dyn2 (Cook et al., 1994; Sontag et al., 1994), and the *shibire* gene product of *D. melanogaster* (*Shi*; Chen et al., 1991; van der Bliek and Meyerowitz, 1991) with nonidentical regions shadowed. Dyn1 peptide sequences selected for the generation of pAbs are shown in boldface and are overlined with asterisks, while regions corresponding to the tripartite GTP-binding domain are boxed. Antibodies MC13 and MC14 were made against a peptide that spans the first GTP-binding motif (amino acids 34–48), MC12 was against a peptide that includes the second GTP-binding motif (amino acids 132–143), and MC62 and MC63 were directed against a region conserved only among the dynamins (amino acids 216–241). Note that all three of the selected regions are nearly identical for the three dynamin proteins.

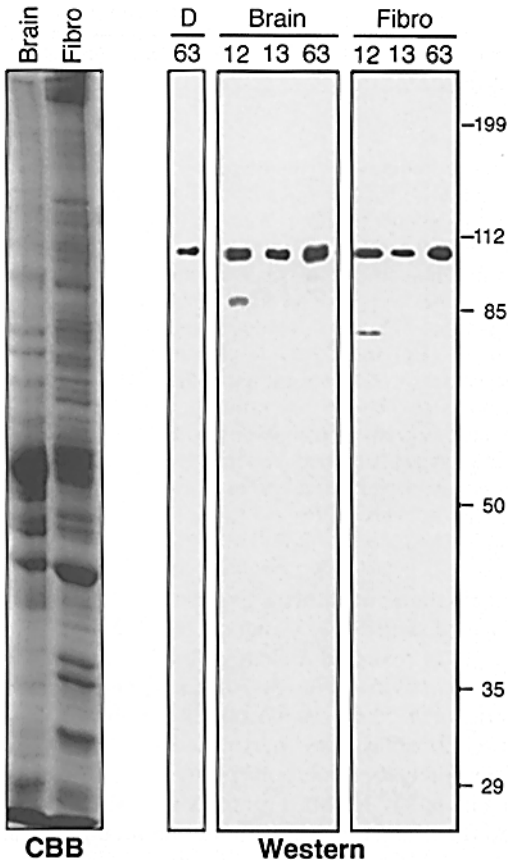

Figure 2. Peptide antibodies recognize purified rat brain dynamin and a protein of identical molecular weight in brain and cultured fibroblasts. Western blot analysis of purified rat brain dynamin (*D*, 0.3 μg/lane), crude protein extracts of rat brain (*Brain*, 45 μg/lane), and cultured human fibroblasts (*Fibro*, 70 μg/lane) probed with peptide antibodies MC12 (12), MC13 (13), and MC63 (63) reveals a major immunoreactive band at 100 kD in each lane. Only MC12 appears to cross-react with an 80–90-kD protein that is detected with much less intensity than the dynamin-immunoreactive band. A corresponding Coomassie-stained gel (*CBB*) shows the total protein profile in the crude extracts of rat brain and cultured human fibroblasts. Despite the large number of different proteins in the crude extracts, the multiple antibodies specifically recognize the dynamin band at 100 kD. MC12 and MC13 also recognize purified rat brain dynamin (data not shown).

shown). The only band consistently recognized among all the antibodies was at 100 kD, while the lower titer MC12 pAb also faintly recognized an 80–90-kD protein in both extracts.

To further test antibody specificity, we did immunoprecipitation studies on total protein extracts from brain and cultured fibroblasts. As seen in the corresponding silver-stained gel (Fig. 3 *A*), the predominant protein precipitated by each antidynamin antibody migrated with purified brain dynamin. Minor bands were also detected in the immunoprecipitations done with irrelevant antibodies. An 85-kD protein was faintly detected in the immunoprecipitate obtained with MC12 only. Fibroblasts were grown to extreme confluency for this study, and were harvested using a prolonged incubation in 0.25% trypsin. Under these conditions, multiple 80–90-kD bands were detected by SDS-PAGE of the immunoprecipitate obtained with MC63 (Fig. 3 *A*), as well as by Western blot analysis of the initial protein extract using either MC63 or an antibody that is specific for the internal region of Dyn2 (data not shown). These bands probably correspond to proteolytic fragments of dynamin since they were recognized by the Dyn2-specific antibody by immunoprecipitation and Western blot analysis (data not shown). To further characterize the proteins in these samples, the immunoprecipitates from the brain were transferred to polyvinyldifluoride membranes and processed for Western blot analysis using antibodies to Dyn1, kinesin, β-COP, and Vps1p. Fig. 3 *B* shows that the prominent 100-kD protein immunoprecipitated by each of the antidynamin pAbs (MC12, MC13, and MC63) was indeed dynamin, as determined by a Dyn1-specific tail antibody. Kinesin was not detected in the antidynamin antibody immunoprecipitates, but was present only in the antikinesin antibody immunoprecipitate and in the crude brain homogenate (Fig. 3 *B*). Likewise, the Golgi-associated coat protein β-COP was not recognized in any of the immunoprecipitates (data not shown). In contrast, mAbs or pAbs to Vps1p did not detect an 80-kD Vps1p band in the immunoprecipitates that was seen in crude yeast extracts. Interestingly, however, the pAb against Vps1p recognized both purified and immunoprecipitated brain dynamin, suggesting a cross-reactivity of this antibody.

To characterize the 100-kD immunoreactive dynamin-like protein that was detected in crude homogenates of both brain and cultured fibroblasts, we tested whether this protein sedimented with membranes and microtubules, as has been demonstrated previously for brain dynamin (Scaife and Margolis, 1990). Brain and fibroblast homogenates were centrifuged at 30,000 *g* to pellet the heavy membrane fractions and the supernatants centrifuged at 170,000 *g* to obtain microsomal pellets and cytosolic fractions. Microtubules that had been assembled from purified bovine brain tubulin were incubated with the cytosolic fractions for 30 min at 37°C and then collected by centrifuging at 170,000 *g*. Fig. 4 shows that substantial amounts of the dynamin-like protein associated with heavy membrane and microsomal fractions from both brain and fibroblasts, while less was found in cytosolic fractions. In addition, the soluble protein pelleted with exogenously added microtubules in the absence of nucleotide. These results indicate that the 100-kD proteins that are recognized by our antidynamin antibodies in both neuronal and nonneuronal cell types are biochemically similar to brain dynamin.

Distribution of Dynamin Immunoreactivity in Cultured Cells

To define the cellular localization of dynamin, we used each of the affinity-purified antidynamin antibodies for indirect immunofluorescence analysis of fixed cells. As shown in Fig. 5, three different antidynamin antibodies (MC12, MC13, and MC63) labeled an elaborate perinuclear membrane network and a population of punctate vesicular structures in cultured human fibroblasts. Similar results were obtained using pAbs MC14 and MC62 (data not shown). Additionally, these localizations were susceptible to harsh detergent extractions, indicating an association

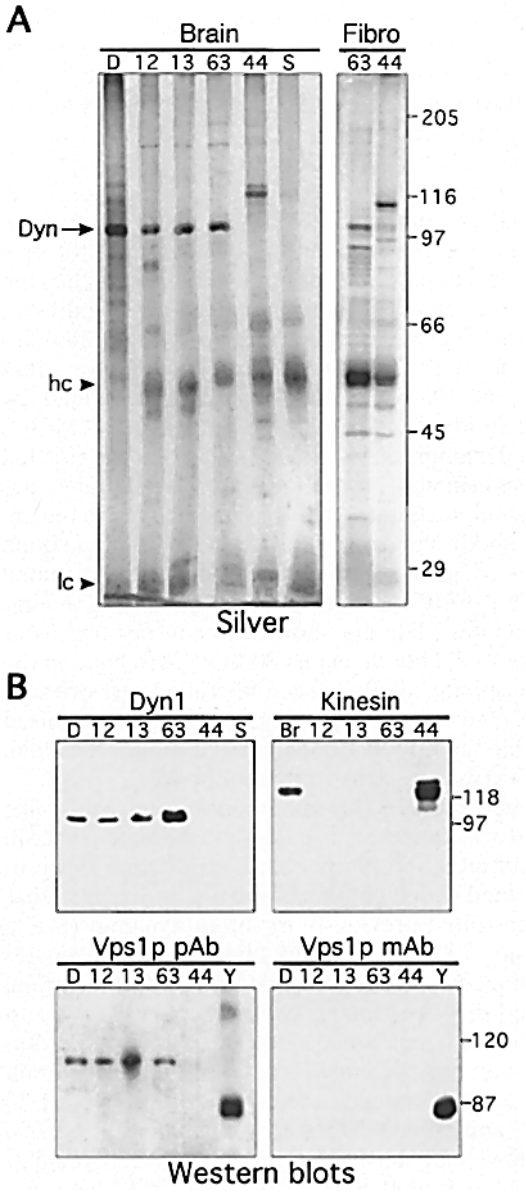

Figure 3. Multiple antibodies specifically immunoprecipitate dynamin. (*A*) A silver-stained gel showing the protein profile of immunoprecipitates obtained from a crude brain extract (*Brain*) with MC12 (*12*), MC13 (*13*), and MC63 (*63*) reveals comigration of a major protein band detected at 100 kD and purified brain dynamin (*D*, *arrow*). This band represents the only protein consistently recognized by the multiple antibodies to dynamin that was not also immunoprecipitated with a pAb to kinesin (*44*) or normal rabbit serum (*S*). Only MC12 immunoprecipitated a protein detected as a minor band at ~80 kD. Proteins were also immunoprecipitated from a fibroblast total protein extract (*Fibro*) using the MC63 and kinesin antibodies. The corresponding silver-stained gel indicates that a protein doublet specifically recognized by MC63 migrates with purified brain dynamin. The less intense bands at 80–90 kD most likely represent proteolytic fragments of dynamin that have been described previously (Hinshaw and Schmid, 1995; Tuma et al., 1993), since these are detected with an antibody that is specific for Dyn2 by Western blot analysis (data not shown). Immunoglobulin heavy (*hc*) and light (*lc*) chains are denoted by arrowheads. (*B*) Proteins immunoprecipitated from the brain were probed with multiple antibodies for Western blot analysis. The Dyn1-specific carboxyl-terminal tail antibody (*Dyn1*) detected purified brain dynamin (*D*) and the major 100-kD protein that was recognized by each of the multiple antibodies to dynamin (*12*, *13*, and *63*). Kinesin was detected only in the lanes containing crude brain extract (*Br*) or an immunoprecipitate obtained with an antibody to kinesin (*44*), and not in the lanes containing immunoprecipitates obtained with the antibodies to dynamin. Interestingly, a pAb to Vps1p not only recognized Vps1p in the crude yeast extract (*Y*), but also detected both purified and immunoprecipitated brain dynamin. A mAb to Vps1p, however, reacted only with the crude yeast extract and not with any of the immunoprecipitated proteins. The corresponding molecular weights are listed to the right of each panel.

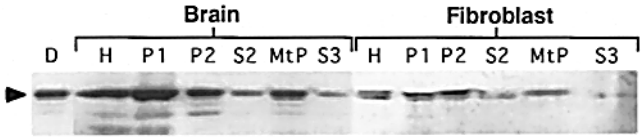

Figure 4. Peptide antibodies to dynamin recognize a 100-kD protein in brain and fibroblast homogenates that sediments with crude membranes and microtubules. Western blot analysis of purified rat brain dynamin (*D*) and subcellular fractions obtained from rat brain and human fibroblasts stained with antidynamin antibody MC63. Lanes were loaded with four times more fibroblast protein than that of brain. Fractions include crude homogenates (*H*), 30,000 *g* (*P1*) and 170,000 *g* (*P2*) membrane pellets, 170,000 *g* supernatants (*S2*), microtubule pellets (*MtP*), and resulting supernatants (*S3*). Note that while there is considerably more dynamin in the brain as compared to fibroblast homogenates, both dynamin proteins behave similarly. Dynamin from both cell types sediments with membranes (*P1* and *P2*) and exogenously added microtubules (*MtP*).

with membranes (data not shown). Double-labeling experiments performed with the Golgi-specific mAb 10E6 (Wood et al., 1991) revealed a clear colocalization of dynamin immunoreactivity (Fig. 5, *a–c*) and the labeled Golgi apparatus (Fig. 5, *a′–c′*). To test if this localization was peculiar to fibroblasts, we performed similar studies on a neural-derived cell population (human melanocytes). As shown in Fig. 6, MC12, MC13, and MC63 also prominently labeled the Golgi apparatus in human melanocytes, as did MC14 and MC62 (data not shown). Because the pAb to Vps1p cross-reacted with dynamin by immunoblot analysis (Fig. 3 *B*), we tested whether it also stained the Golgi apparatus in cultured cells. Remarkably, this anti-Vps1p pAb strongly labeled the Golgi apparatus in human fibroblasts (Fig. 7), while no immunoreactivity was detected with the anti-Vps1p mAb (data not shown). We find it significant that this pAb gives a staining pattern identical to that observed with the multiple antidynamin antibodies.

Although the mAb 10E6 has been previously shown to specifically label Golgi compartments (Wood et al., 1991), late endosomes and lysosomes often have a perinuclear distribution and may be confused with the Golgi apparatus. Therefore, we double labeled cultured human fibroblasts for dynamin and late endosomes/lysosomes. Fibroblasts were allowed to take up FITC-conjugated dextran for 3.5 h in culture, were incubated an additional 35 min in the absence of dextran, and were then processed for indirect immunocytochemistry to visualize dynamin using a TRITC-conjugated secondary antibody. As shown in Fig. 8, dynamin immunoreactivity was detected as a reticular

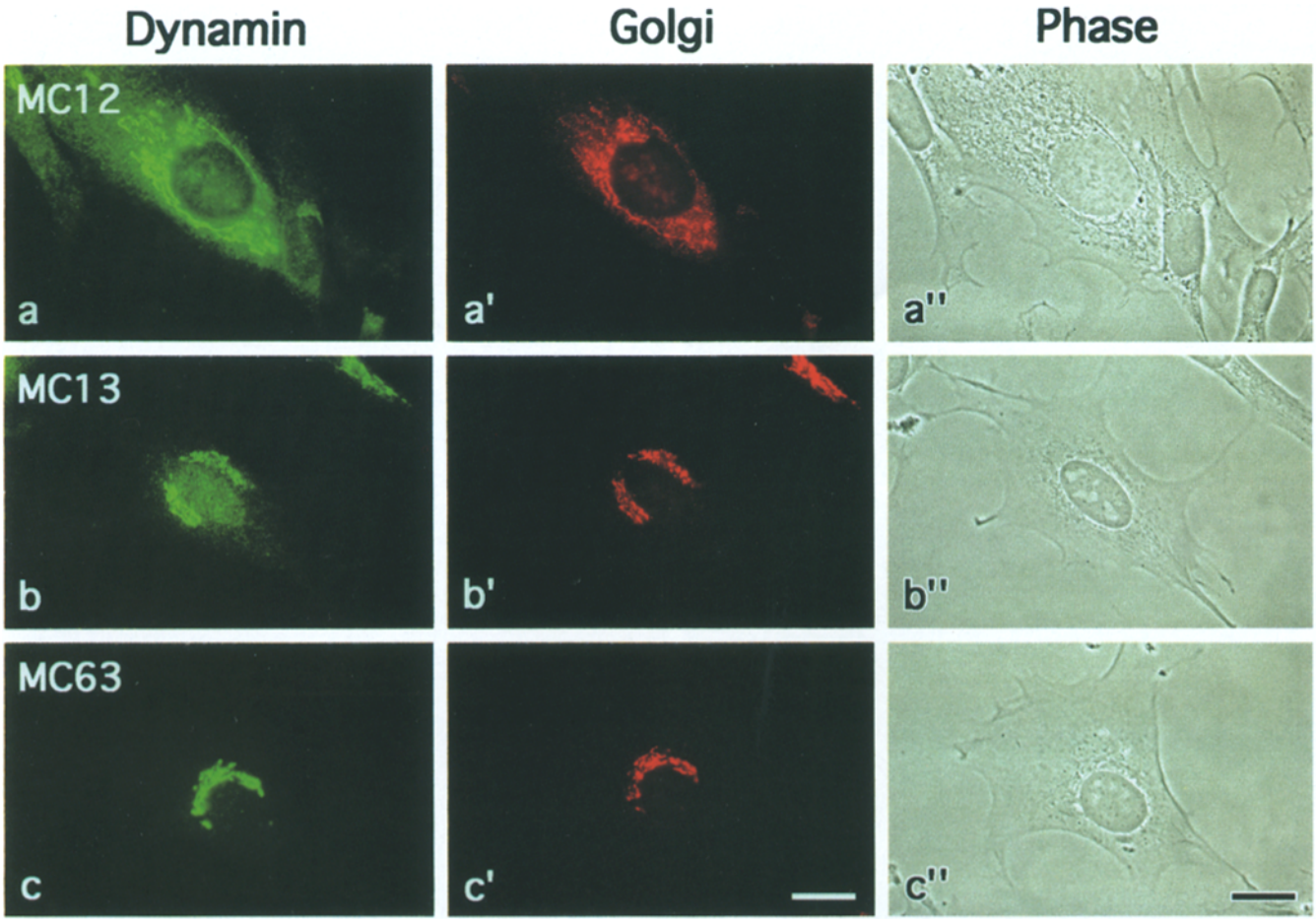

Figure 5. Multiple antibodies to dynamin label the Golgi apparatus in fibroblasts. Cultured human fibroblasts were processed for double-label immunofluorescence microscopy using three different affinity-purified antibodies to dynamin: MC12 (*a*), MC13 (*b*), and MC63 (*c*). (*a'*–c') The Golgi-specific mAb 10E6. Note the strong colocalization of dynamin immunoreactivity (*green*) and the Golgi apparatus (*red*). Identical staining patterns are seen with two other antidynamin antibodies (MC14 and MC62) not shown. In addition to the Golgi stain, punctate vesicular structures are also seen. No immunofluorescence staining was detected when preimmune sera or void volumes from the antibody affinity purification step were used (data not shown). (*a''*–c'') Corresponding phase contrast images. Bars, 20 μm.

Golgi structure, while late endosomes and lysosomes appeared as punctate vesicles that had a wider distribution than and shared little overlap with the dynamin label. Because early recycling endosomal compartments may have a perinuclear distribution, cells were also fixed immediately after incubation with fluorescently labeled dextran or transferrin before dynamin staining. In these preparations, we observed little, if any, overlap between dynamin and the labeled markers, indicating that they localize to distinct compartments.

Membrane-associated Dynamin Is Enriched in Subcellular Golgi Fractions

To support the morphological observations indicating that a dynamin-like protein associated with the Golgi apparatus, we used Western blot analysis to test for dynamin immunoreactivity on Golgi membrane fractions isolated from rat liver. We used three separate protocols, including those of Hamilton and co-workers (1991), Leelavathi et al. (1970), as modified by Fath et al. (1994), and Howell and Palade (1982), as described in Marks et al. (1994), to obtain preparations of Golgi membranes enriched significantly over those present in whole tissue homogenates. Because the results obtained by these methods were similar, only those from the modified Leelavathi preparation are shown here. With this method, we obtained a postnuclear supernatant, a total membrane pellet, a crude initial membrane fraction, a highly enriched mixed Golgi fraction, and fractions containing either Golgi vesicles or Golgi stacks. These subcellular fractions were immunoblotted (Fig. 9 *A*) for dynamin and several organelle marker proteins including α-mannosidase II (Moremen et al., 1991), β-COP (Allen and Kreis, 1986), and rab 6 (Goud et al., 1990) for the Golgi apparatus, and ribophorin II for the RER (Hortsch et al., 1986). As demonstrated in Fig. 9 *A* and Table I, which are representative of multiple experiments, both the dynamin immunoreactivity and the immunoreactivity for the different Golgi-associated proteins increased significantly in the stacked Golgi fraction compared to the total membrane fraction. In contrast, the RER-associated ribophorin II was significantly deenriched in this fraction. As shown in the corresponding electron micrographs (Fig. 9, *B* and *C*), this stacked Golgi

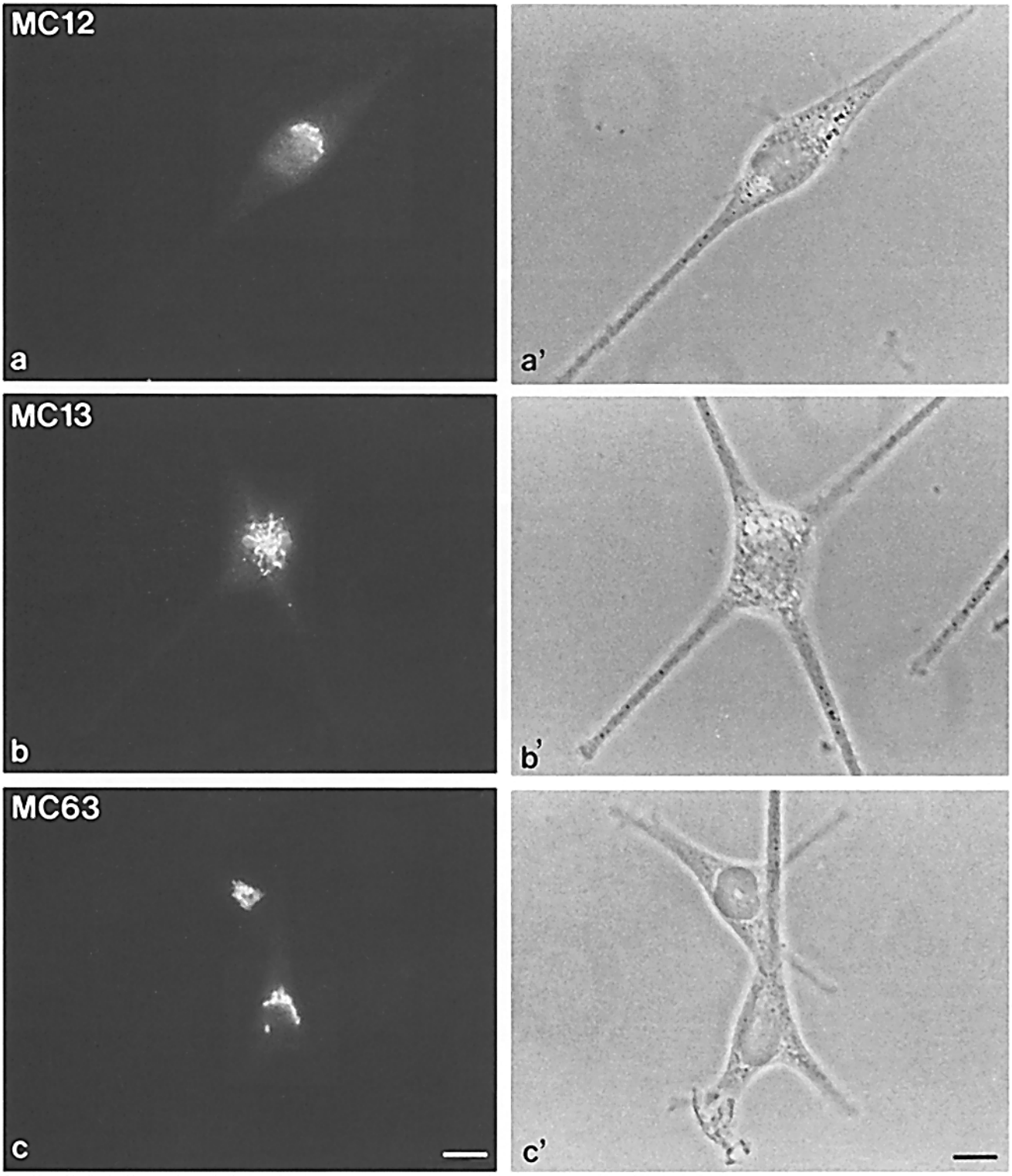

Figure 6. Dynamin immunoreactivity on the Golgi apparatus in melanocytes. Cultured human melanocytes were processed for indirect immunofluorescence microscopy as was done for the fibroblasts in Fig. 5. Antidynamin antibodies MC12 (*a*), MC13 (*b*), and MC63 (*c*) all label the Golgi apparatus. No staining was observed when preimmune sera were used (data not shown). (*a'*–*c'*) Corresponding phase-contrast images. Bars, 10 μm.

fraction is replete with Golgi cisternae as well as coated buds and lipoprotein-containing vesicles that are characteristic of Golgi membranes. Despite the substantial enrichment of Golgi membranes in this fraction, it was important to define the amount of endocytic components that were present, since dynamin has been observed to associate with plasmalemmal coated pits and membrane invaginations. To this end, we immunoblotted all Golgi frac-

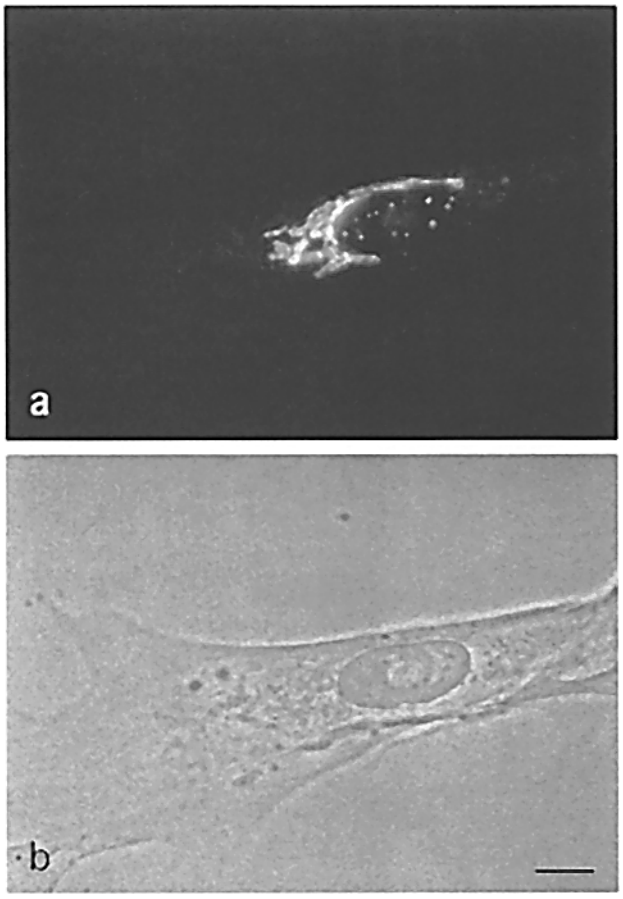

Figure 7. The Golgi apparatus in fibroblasts is labeled with a pAb to Vps1p. Cultured human fibroblasts were processed for indirect immunofluorescence microscopy using a pAb to Vps1p that cross-reacts with dynamin (Fig. 3 *B*). (*a*) This antibody strongly labels the Golgi apparatus. No staining was detected using an mAb to Vps1p (data not shown). (*b*) Corresponding phase-contrast image. Bar, 20 μm.

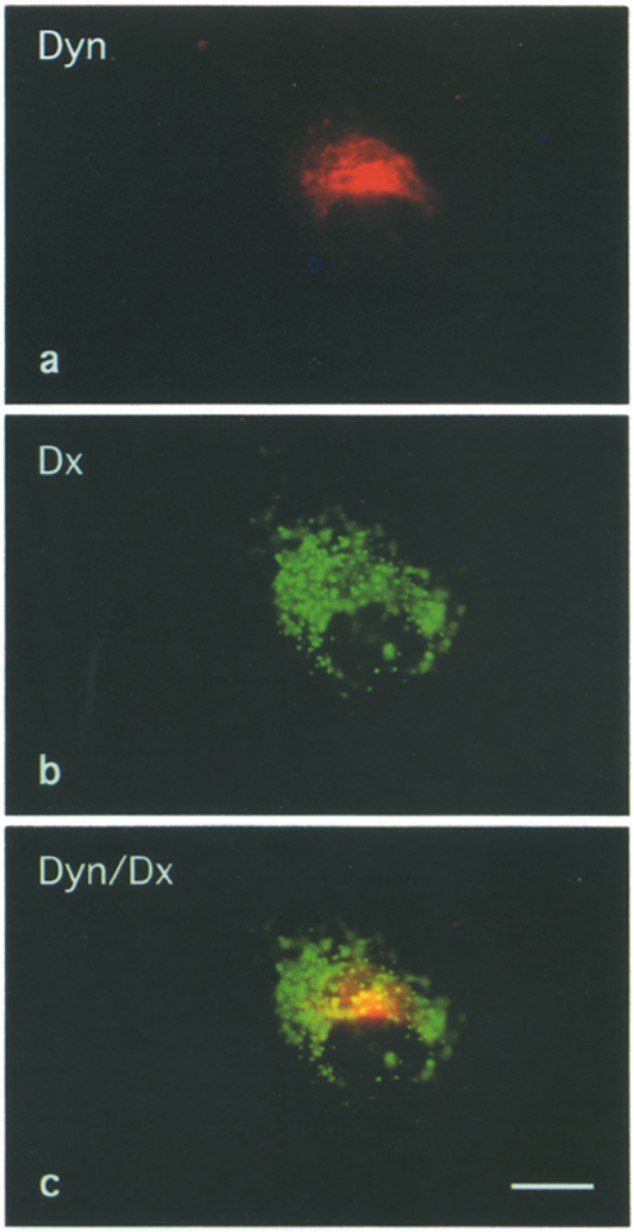

Figure 8. Dynamin immunoreactivity in fibroblasts does not localize with late endosomes and lysosomes. Cultured human fibroblasts were incubated with FITC-conjugated dextran to label late endosomes and lysosomes (see Materials and Methods) before fixing and processing for indirect immunocytochemistry with the antidynamin antibody MC63. (*a* and *c*) Dynamin immunoreactivity detected with a TRITC-conjugated secondary antibody labels the Golgi apparatus (*red*). (*b* and *c*) Internalized dextran in late endosomes and lysosomes (*green*). Note that there is little overlap between the two signals (*c, yellow*). No qualitative differences in the dextran labeling were observed as a result of immunocytochemical processing (data not shown). Bar, 15 μm.

tions with a pAb to the polymeric IgA receptor. This protein has been used as a marker to study the maturation and posttranslational processing of proteins in the hepatic secretory and endocytic pathways (e.g., Sztul et al., 1985; Larkin et al., 1986). The 105-, 116-, and 120-kD forms of this receptor represent its passage through the RER and early Golgi, the Golgi, and plasma membrane and endocytic compartments, respectively. While the endocytic 120-kD form of the polymeric IgA receptor was present in all the Golgi fractions, it was not enriched in the stacked Golgi fraction as compared to the crude initial membrane fraction. There was a significant enrichment (more than sixfold), however, of the immature RER/Golgi form of the receptor in this stacked Golgi fraction. Thus, while putative endosomal compartments may contaminate all fractions to some extent, dynamin-enrichment parallels an increase in the secretory form of the polymeric IgA receptor.

To confirm the association of a dynamin-like protein with Golgi membranes, we isolated dynamin-immunoreactive membranes from subcellular Golgi fractions obtained from liver. Fractions enriched in Golgi membranes were prepared by two different methods, including that used to obtain the stacked Golgi fraction as discussed above and one used by Howell and Palade (1982) to obtain a sample enriched in Golgi heavy and Golgi light fractions, as described previously (Marks et al., 1994). These fractions were incubated with superparamagnetic beads that had been precoated with either antidynamin antibody MC63

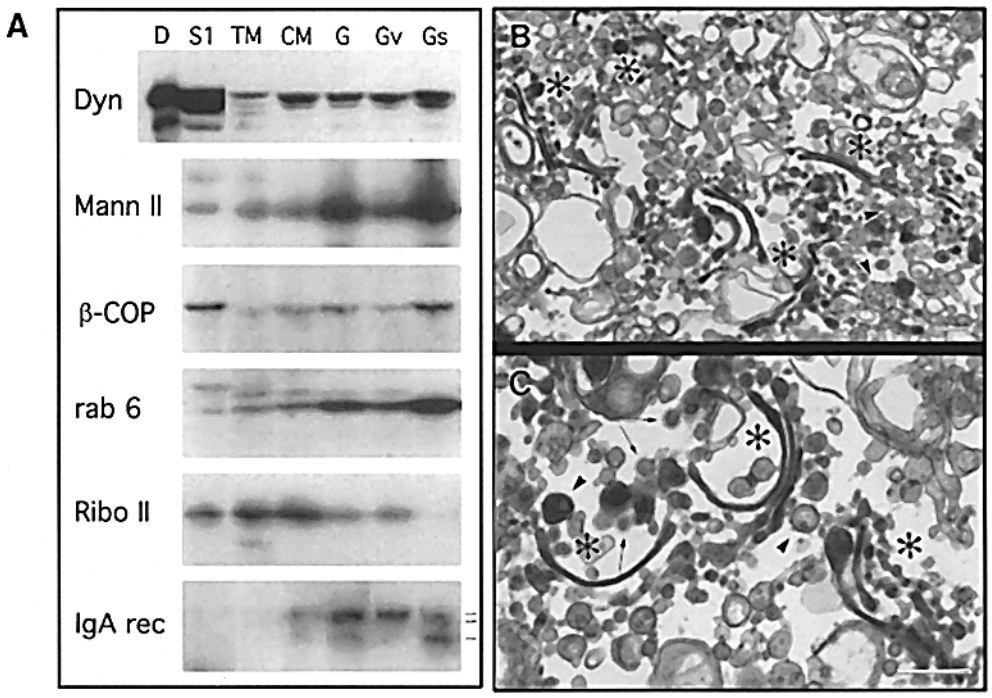

Figure 9. Dynamin is enriched in subcellular Golgi fractions, as indicated by Western blot analysis. (*A*) Antidynamin antibody MC63 was used for Western blot analysis of subcellular fractions from liver representing various stages of Golgi purification. These fractions include a postnuclear supernatant (*S1*), a total membrane pellet (*TM*), a crude membrane fraction (*CM*) obtained from the first discontinuous sucrose gradient centrifugation, and a mixed Golgi fraction (*G*) obtained after a second discontinuous sucrose gradient centrifugation. Highly enriched fractions containing Golgi vesicles (*Gv*) or intact Golgi stacks (*Gs*) were obtained upon further subfractionation of the mixed Golgi fraction (see Materials and Methods). Fractions were characterized using antibodies against three different Golgi marker proteins, α-mannosidase II (*Mann II*), β-COP, and rab 6; the RER-associated protein, ribophorin II (*Ribo II*); and the polymeric IgA receptor (*IgA rec*). A dynamin-immunoreactive band that is detected in the postnuclear supernatant migrates with purified brain dynamin (*D*, 1 μg/lane). This dynamin-immunoreactive protein is deenriched in the total membrane pellet, indicating that it does not preferentially associate with membranes. Upon enriching for Golgi membranes, as determined by the increased immunoreactivity for α-mannosidase II, β-COP, rab 6, and the 105-kD form of the polymeric IgA receptor (*IgA rec, lower band*), there is a concomitant increase in dynamin immunoreactivity, with the greatest enrichment in the stacked Golgi fraction. This stacked Golgi fraction has little ribophorin II immunoreactivity, indicating that the RER is not enriched. Also, note that there is no increase in the immunoreactivity for the 120-kD form of the polymeric IgA receptor (IgA rec 120, *upper band*), indicating that endocytic compartments, likewise, are not enriched in this stacked Golgi fraction. Lines to the lower right of the panel indicate the positions, from top to bottom, of the 120-, 116-, and 105-kD forms of the polymeric IgA receptor, respectively. An equal amount of protein was loaded for each liver fraction (50 μg/lane). (*B* and *C*) Electron micrographs demonstrating numerous Golgi profiles in the isolated stacked Golgi fraction, including stacked Golgi elements (*asterisks*) and lipoprotein-containing vesicles (*arrowheads*). Coated buds and vesicles can also be seen (*C, small arrows*). Bars, 0.3 μm.

or an anti–rabbit IgG linker antibody alone as a control. Thus, only organellar membranes that associated with dynamin would bind specifically to the MC63-coated beads. Beads and associated membranes were then collected with a magnet as the immunoisolated fractions, while any material remaining in the supernatants was centrifuged and collected as the unbound fractions. All fractions were subjected to Western blot analysis using antibodies to the Golgi protein α-mannosidase II and to dynamin, or they were fixed and prepared for EM. We found that α-mannosidase II was enriched significantly in the immunoisolated fractions and little remained in the unbound fractions (Fig. 10 *A*), indicating that most of the Golgi membranes present in the starting material were isolated. As anticipated, the 100-kD dynamin-like protein was also recognized in the immunoisolated fractions, with little detected in the unbound fractions. In contrast, the peripheral plasma membrane protein α-adaptin, although present in the starting membrane fractions, was not detected in the immunoisolated fractions (data not shown). Only low levels of immunoreactivity for α-mannosidase II or dynamin were found in the isolated fractions obtained with control beads (data not shown). This indicates that the beads coated with antidynamin antibody were not pulling down Golgi mem-

Table I. Quantitation of Dynamin and Organelle Marker Protein Immunoreactivity in Subcellular Fractions Isolated from Liver

	Subcellular Fraction			
Protein	TM	CM	G	Gs
Dynamin	1.0	1.7	1.8	5.1
Man II	1.0	1.4	3.1	3.8
β-COP	1.0	2.6	2.8	5.3
Rab 6	1.0	1.8	7.9	15.6
Rib II	1.0	1.2	0.4	0
IgA rec 120*		1.0	3.3	1.0
IgA rec 116*		1.0	3.6	2.2
IgA rec 105*		1.0	2.9	6.5

Subcellular fractions isolated from rat liver were analyzed by Western blotting as in Fig. 9 and for densitometry as described in Materials and Methods. TM, total membrane fraction; CM, crude initial membrane fraction; G, mixed Golgi fraction; Gs, stacked Golgi fraction; Mann II, α-mannosidase II; Rib II, ribophorin II; and IgA rec 120, 116, and 105 represent the 120-kD (plasma membrane/endosomal), 116-kD (late Golgi), and 105-kD (RER/early Golgi) forms of the polymeric IgA receptor, respectively. Relative densitometric values for each fraction were normalized to the total membrane fraction and are represented as -fold increase.

*Since little polymeric IgA receptor immunoreactivity was detected in the total membrane fraction, relative values were normalized to the crude initial membrane fraction.

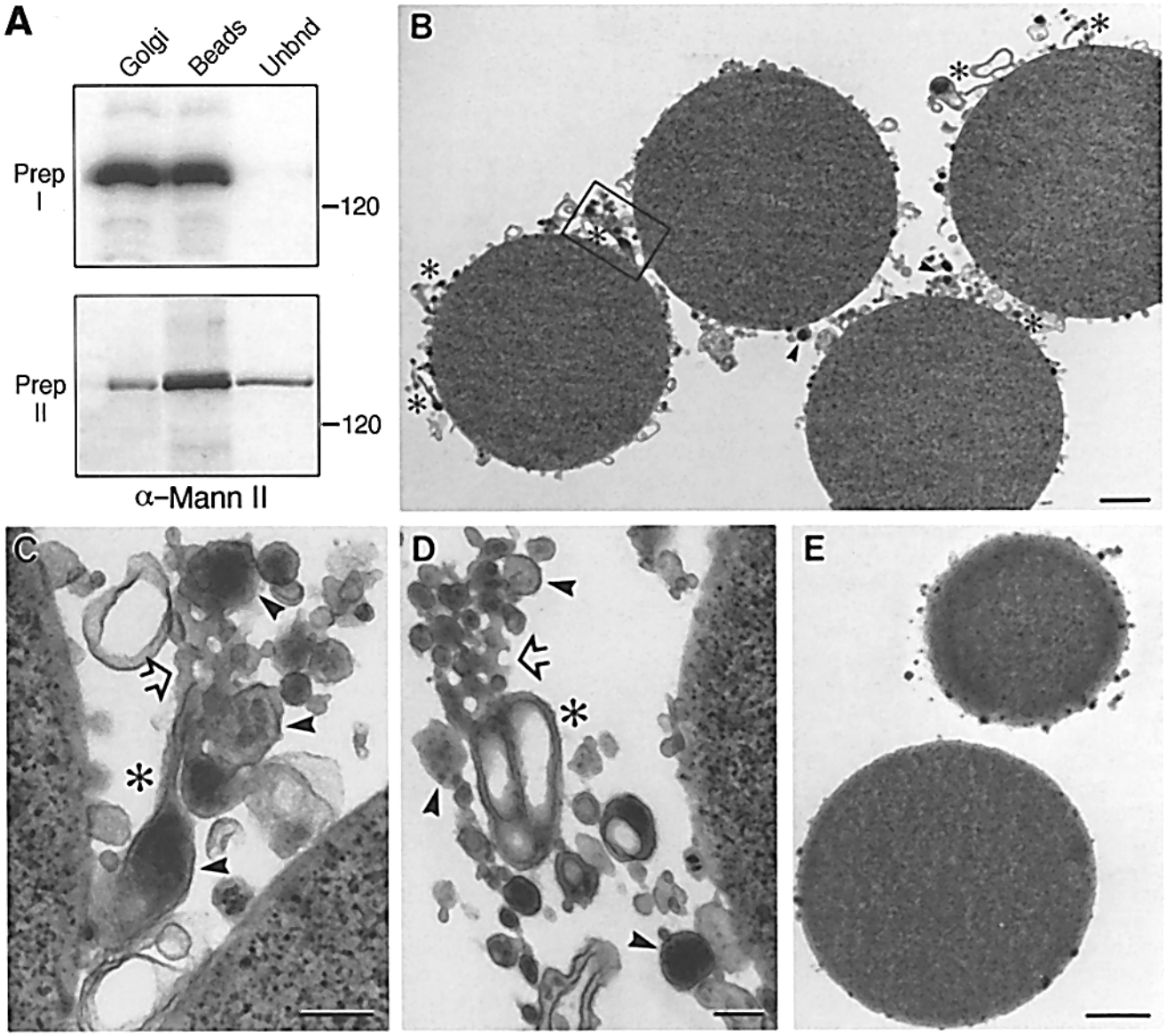

Figure 10. Golgi membranes are immunoisolated using an antibody to dynamin. (*A*) Starting and immunoisolated fractions were analyzed by immunoblotting with an antibody to the Golgi protein α-mannosidase II. Golgi fractions (*Golgi*) were isolated from liver using two different established methods, and consisted of either a stacked Golgi fraction (*Prep I*), or a mixture of Golgi heavy and Golgi light membrane fractions (*Prep II*; see Materials and Methods). These fractions were incubated with beads that were coated with affinity-purified antibody MC63, and the material that bound (*Beads*) or did not bind (*Unbnd*) to the beads was collected. Protein loads were equivalent to the starting Golgi fraction for each lane. There was a significant accumulation of the Golgi marker protein in the immunoisolated bead fractions, while very little remained in the unbound fractions. (*B–D*) Electron micrographs representative of the immunoisolated fraction obtained from the stacked Golgi fraction with antibody MC63-coated beads, as described above. Multiple Golgi profiles (*asterisks*), lipoprotein-containing vesicles (*arrowheads*), and fenestrated membranes associated with Golgi elements (*C* and *D*, *open arrows*) are clearly visible. (*E*) Electron micrograph representative of a control fraction obtained after incubating the stacked Golgi fraction with beads that were coated with an anti–rabbit IgG linker antibody alone. Dark granules are noncellular debris. Few, if any, membranes are associated with the beads. Bars, 0.6 μm (*B* and *E*) and 0.15 μm (*C* and *D*).

branes indiscriminately, but recognized a specific dynamin antigen associated with the Golgi cisternae. As shown in the corresponding electron micrographs, the morphology of the immunoisolated membranes is consistent with that of Golgi (Fig. 10, *B–D*) including numerous cisternae, fenestrations, and lipoprotein-containing vesicles. In contrast, isolations obtained with control beads were devoid of membranes (Fig. 10 *E*). These results confirm that a dynamin-like protein is present on Golgi membranes.

Discussion

A Dynamin-related Protein on the Golgi Apparatus

In this study, we have used multiple pAbs made to distinct sites of dynamin to determine its cellular distribution by indirect immunofluorescence microscopy of cultured cells. In addition, we have performed Western blot and EM analysis of both Golgi-enriched and dynamin-immunore-

active membrane fractions isolated from the liver. These pAbs were directed against synthetic peptides representing three different regions conserved within the dynamin family of proteins (Fig. 1) and should recognize all of the known dynamin isoforms. By Western blot analysis (Fig. 2) and immunoprecipitation studies (Fig. 3), we show that these pAbs are both sensitive and specific for dynamin. These pAbs react with a 100-kD protein in fibroblasts that has similar biochemical properties to brain dynamin, such as binding and pelleting with membrane fractions and assembled microtubules in vitro (Fig. 4). We assume that this immunoreactive protein is Dyn2, which is found in all tissues (Cook et al., 1994; Sontag et al., 1994), since the other dynamin isoforms are restricted to neural tissues and testis (Nakata et al., 1991, 1993; Cook et al., 1994; Sontag et al., 1994).

The immunocytochemical studies described here indicate that dynamin has two prominent localizations in the cell populations examined. These include a ubiquitous, punctate staining of the cytoplasm that is generally consistent with the observations of others (Scaife and Margolis, 1990; Herskovits et al., 1993*a*; Noda et al., 1993; Gass et al., 1995) and unexpectedly, a marked staining of the Golgi apparatus, as confirmed by double-labeling studies with a Golgi-specific mAb (Fig. 5). This Golgi localization is striking and observed consistently in all the cell types examined using several different affinity-purified antidynamin antibodies (Figs. 5 and 6). Most often, both of these staining patterns are seen concomitantly in the same cell, indicating that the recognized antigen may have a differential distribution. These morphological observations are reinforced further through Western blot analysis of subcellular fractions isolated from the liver (Fig. 9). Although prevalent in a cytosolic fraction, the amount of a 100-kD dynamin-immunoreactive protein in a highly enriched Golgi membrane fraction is increased more than fivefold when compared to a total membrane fraction (Table I). This result argues that the association of this dynamin-like protein with the Golgi fraction is physiological and does not represent random sticking to membranes. We find it significant that this enrichment of membrane-associated dynamin parallels the enrichment of several different Golgi-associated proteins in this same fraction. Furthermore, only dynamin is recognized in this enriched Golgi fraction, which is replete with other associated GTP-binding proteins. A concern with any subcellular fractionation procedure is that an isolated fraction may be comprised of vesiculated membranes from multiple types of organelles. It is for this reason that we have used three separate methods to obtain fractions enriched in Golgi marker proteins and show that dynamin is coenriched in each of these fractions over a total membrane fraction. Furthermore, we have used an antibody to the polymeric IgA receptor to show that the 120-kD plasmalemmal/endosomal form of this receptor is not enriched in these Golgi membrane preparations. To confirm that it is Golgi and not other membranes that are responsible for the dynamin enrichment in these fractions, we immunoisolated membranes using beads coated with the sensitive and specific antidynamin antibody MC63. Substantially, these MC63-coated beads bound to Golgi elements, as determined both biochemically and morphologically (Fig. 10). Since MC63 specifically immunoprecipitated dynamin from total protein extracts of brain, fibroblasts, and liver (Fig. 3 and data not shown), and since Western blot analysis of subcellular Golgi fractions indicated this antibody reacted with only a single 100-kD protein that migrated with purified dynamin (Fig. 9), we are convinced that a dynamin-like protein is localized to the Golgi apparatus.

Although this is the first description of a dynamin-related protein associated with the Golgi apparatus in mammalian cells, Vps1p localizes to the Golgi in yeast, where it performs an essential function in sorting proteins destined for the vacuole (Rothman et al., 1990; Vater et al., 1992; Wilsbach and Payne, 1993). Because the amino-terminal domains of dynamin and Vps1p share 45% identity (Obar et al., 1990), it is possible that the antibodies to dynamin used in this study also recognize a mammalian Vps1p homologue. To address this, we immunoprecipitated proteins from brain protein extracts using each antidynamin antibody (MC12, MC13, and MC63) and analyzed the immunoprecipitates by SDS-PAGE and by immunoblotting with mAbs and pAbs to Vps1p. Each of the antidynamin antibodies immunoprecipitated a 100-kD protein that was recognized by a Dyn1 tail–specific antibody, indicating that this protein is indeed dynamin. In addition, the pAb to Vps1p recognized both purified brain dynamin and the immunoprecipitated dynamin (Fig. 3). In contrast, the mAb to Vps1p did not react with any immunoprecipitated protein. Remarkably, the anti-Vps1p pAb also strongly labeled the Golgi apparatus in cultured human fibroblasts (Fig. 7), whereas the anti-Vps1p mAb did not (data not shown). This provides a provocative correlation between antibodies that react with dynamin by Western blot analysis and those that label the Golgi apparatus in cultured cells by indirect immunofluorescence. The extensive characterization studies detailed here indicate that the antidynamin antibodies used in this study are specific for the dynamins, although we cannot exclude the possibility that other closely related members of the dynamin family are also recognized. Nonetheless, these results provide novel and important evidence that a dynamin-like protein is present on the Golgi apparatus in mammalian cells.

Because of the predicted endocytic function of dynamin, we were surprised to find dynamin localized to the Golgi (Figs. 5 and 6), and not endosomes and lysosomes (Fig. 8), or with clathrin at the plasma membrane (data not shown). Furthermore, immunofluorescence studies of cultured cells by others have reported a diffuse granular stain (Scaife and Margolis, 1990; Herskovits et al., 1993*a*), and a punctate, vesicular localization (Scaife and Margolis, 1990; Herskovits et al., 1993*a*; Faire and Bonder, 1993; Noda et al., 1993; Damke et al., 1994, 1995). We believe there are at least two explanations for these contrasting results. First, it is likely that the many antidynamin antibodies currently available differ in their ability to recognize endogenous dynamin. For example, we are aware of only one antibody to dynamin that localizes with clathrin and labels membrane invaginations at the cell surface (Damke et al., 1994; Takei et al., 1995). A similar situation exists for the numerous antibodies generated against the microtubule-associated motor enzyme kinesin, in which only a few have been shown to consistently stain vesicular compartments (e.g., Pfister et al., 1989; Henson et al., 1992; Marks et al.,

1994; Schmitz et al., 1994). Interestingly, only two of these antibodies have been reported to stain the *trans*-Golgi network (Marks et al., 1994; Schmitz et al., 1994), while a third does not (Leopold et al., 1992). Thus, while each of these characterized antibodies recognize kinesin by biochemical criteria, they produce very different immunocytochemical localizations. A second explanation is that there are multiple dynamin genes (Obar et al., 1990; Nakata et al., 1993; Cook et al., 1994; Sontag et al., 1994) with two separate alternatively spliced regions in both the neuronal-specific Dyn1 and the ubiquitously expressed Dyn2, resulting in the potential expression of four isoforms of each gene (Sontag et al., 1994). It is likely that dynamin isoforms are differentially distributed and perform related, yet distinct functions. A case in point is the kinesin superfamily in which different isoforms appear to associate with different cytoplasmic organelles (e.g., Hall and Hedgecock, 1991; Nangaku et al., 1994; Okada et al., 1995). Another relevant example is a heterotrimeric GTP-binding protein α subunit that contains an alternatively spliced carboxyl terminus that changes its localization from the plasma membrane to the Golgi apparatus (Montmayeur and Borrelli, 1994). Finally, a differential localization may be explained by differences between species, cell populations, or posttranslational modifications near the antigenic sites.

Correlating Dynamin Localization with Function

Along with a predicted endocytic function, the *shibire* gene product in *D. melanogaster* has been proposed to play a role in other cell processes including cell adhesion, growth cone formation, neurite extension and elongation, as well as cell differentiation (Buzin et al., 1978; Kim and Wu, 1987; Poodry, 1990). It is unknown whether dynamin participates in this wide variety of cellular processes directly or via endocytic mechanisms. The morphological and biochemical observations presented here provide support for additional functions of the dynamin family through interactions with membranous organelles distinct from the endocytic pathway. Although unanticipated, the association of dynamin with the secretory pathway is supported by several previous observations made by others. For example, Western blot analysis of membrane fractions from the brain detected dynamin in fractions containing crude microsomes and synaptic vesicles (Noda et al., 1993; Tuma et al., 1993). Interestingly, EM of dynamin-enriched membrane fractions from rat brain showed a population of smooth, vesiculated membranes devoid of clathrin coats (Scaife and Margolis, 1990). In addition, a study examining the distribution of dynamin in ligated nerves showed an accumulation of dynamin on the proximal side of the ligation, where outward moving secretory vesicles collect (Noda et al., 1993). Antidynamin antibodies also strongly stained the cortical secretory granules in sea urchin eggs (Faire and Bonder, 1993). It is not yet known whether dynamin actively participates in the secretory pathways of these cells or simply acts as "passive cargo" that is moved toward the plasma membrane to aid in membrane retrieval and endocytosis.

The observations reported here, together with the results of others, provide provocative evidence that dynamins may interact with multiple membrane systems and vesicular pathways. It is attractive to speculate that, as proposed by Kelly (1995), different dynamin-like proteins may perform similar vesicle-budding or protein-sorting functions at both the plasma membrane and Golgi complex. Such a prediction is consistent with many other proteins such as ADP ribosylation factors (Peters et al., 1995; for reviews see Donaldson and Klausner, 1994; Welsh et al., 1994), clathrin (for reviews see Riezman, 1993; Robinson, 1994), adaptins (for reviews see Schmid, 1992; Robinson, 1994), and caveolin (Dupree et al., 1993; Smart et al., 1994; for review see Kurzchalia et al., 1994), which are believed to mediate vesicle budding and fusion events at the plasma membrane and the Golgi apparatus. It is certainly attractive to compare the dynamins with the adaptins that are involved in the formation of clathrin-coated vesicles, both at the cell surface during endocytosis (α and β adaptins), and at the Golgi apparatus during secretion (γ and β′ adaptins). Thus, like adaptins, the dynamins could participate in clathrin-mediated events at two cellular locations. How the different isoforms of dynamin may interact with these membrane systems needs to be defined. Future studies testing the function of dynamins in cell-free Golgi transport assays will certainly prove to be both interesting and insightful.

Primary cultures of human melanocytes and fibroblasts were kindly provided by the laboratory of Dr. M. Pittelkow. Antibodies were obtained as gracious gifts from Drs. F. Brodsky, W. Brown, E. Conibear, M. Gist Farquhar, B. Goud, D. Meyer, and T. Stevens, and purified brain dynamin was a gift from Dr. G. Waters. Special thanks to Ms. T. Cook, K. Kotz, Drs. J. Larkin and D. Marks, and Mr. D. Zacharias for critical reading of the manuscript and for providing helpful comments and discussions. Dr. J. Larkin was also instrumental in establishing the immunoisolation procedure used for this study. We thank Mr. K. Hsaio, E. Krueger, and Mrs. B. Oswald for providing expert technical assistance.

This study was funded by National Institutes of Health grant DK44650 to M.A. McNiven.

Received for publication 30 June 1995 and in revised form 22 February 1996.

References

Allen, V.J., and T.E. Kreis. 1986. A microtubule-binding protein associated with membranes of the Golgi Apparatus. *J. Cell Biol.* 103:2229–2239.

Ames, B.N. 1966. Assay of inorganic phosphate, total phosphate and phosphatases. *Methods Enzymol.* 8:115–118.

Buzin, C.H., S.A. Dewhurst, and R.L. Seecof. 1978. Temperature sensitivity of muscle and neuron differentiation in embryonic cell cultures from the *Drosophila* mutant, *shibire*. *Dev. Biol.* 66:442–456.

Chen, M.S., R.A. Obar, C.C. Schroeder, T.W. Austin, C.A. Poodry, S.C. Wadsworth, and R.B. Vallee. 1991. Multiple forms of dynamin are encoded by *shibire*, a *Drosophila* gene involved in endocytosis. *Nature (Lond.).* 351:583–586.

Chen, M.S., C.C. Burgess, R.B. Vallee, and S.C. Wadsworth. 1992. Developmental stage- and tissue-specific expression of *shibire*, a *Drosophila* gene involved in endocytosis. *J. Cell Sci.* 103:619–628.

Cook, T.A., R. Urrutia, and M.A. McNiven. 1994. Identification of dynamin 2, an isoform ubiquitously expressed in rat tissues. *Proc. Natl. Acad. Sci. USA.* 91:644–648.

Costello, W.J., and L.B. Salkoff. 1986. Suppression of the membrane defect by divalent cations in the *Drosophila* mutant *shibire*. *J. Neurosci.* 6:3634–3639.

Damke, H., T. Baba, D.E. Warnock, and S.L. Schmid. 1994. Induction of mutant dynamin specifically blocks endocytic coated vesicle formation. *J. Cell Biol.* 127:915–934.

Damke, H., T. Baba, A.M. van der Bliek, and S.L. Schmid. 1995. Clathrin-independent pinocytosis is induced in cells overexpressing a temperature-sensitive mutant of dynamin. *J. Cell Biol.* 131:69–80.

Donaldson, J.G., and R.D. Klausner. 1994. ARF: a key regulatory switch in membrane traffic and organelle structure. *Curr. Opin. Cell Biol.* 6:527–532.

Dupree, P., R.G. Parton, G. Raposo, T.V. Kurzchalia, and K. Simons. 1993. Caveolae and sorting in the trans-Golgi network of epithelial cells. *EMBO (Eur.*

Mol. Biol. Org.) J. 12:1597–1605.
Faire, K., and E.M. Bonder. 1993. Sea urchin egg 100-kDa dynamin-related protein: identification of and localization to intracellular vesicles. *Dev. Biol.* 159:581–594.
Fath, K.R., G.M. Trimbur, and D.R. Burgess. 1994. Molecular motors are differentially distributed on Golgi membranes from polarized epithelial cells. *J. Cell Biol.* 126:661–675.
Gammie, A.E., L.J. Kurihara, R.B. Vallee, and M.D. Rose. 1995. *DNM1*, a dynamin-related gene, participates in endosomal trafficking in yeast. *J. Cell Biol.* 130:553–566.
Gass, G.V., J.J.-C. Lin, R. Scaife, and C.-F. Wu. 1996. Two isoforms of *Drosophila* dynamin in wild-type and *shibire*^{ts} neural tissue: different subcellular localization and association mechanisms. *J. Neurogenet.* In press.
Gelfand, V.I., F.K. Gyoeva, V.A. Rosenblat, and N.A. Shanina. 1978. A new ATPase in cytoplasmic microtubule preparations. *FEBS Lett.* 88:197–200.
Goud, B., A. Zahraoui, A. Tavitian, and J. Saraste. 1990. Small GTP-binding protein associated with Golgi cisternae. *Nature (Lond.).* 345:553–556.
Gout, I., R. Dhand, I.D. Hiles, M.J. Fry, G. Panayotou, P. Das, O. Truong, N.F. Totty, J. Hsuan, G.W. Booker, I.D. Campbell, and M.D. Waterfield. 1993. The GTPase dynamin binds to and is activated by a subset of SH3 domains. *Cell.* 75:25–36.
Hall, D.H., and E.M. Hedgecock. 1991. Kinesin-related gene *unc-104* is required for axonal transport of synaptic vesicles in *C. elegans. Cell.* 65:837–847.
Hamilton, R.L., A. Moorehouse, and R.J. Havel. 1991. Isolation and properties of nascent lipoproteins from highly purified rat hepatocytic Golgi fractions. *J. Lipid Res.* 32:529–543.
Henson, J.H., D. Nesbitt, B.D. Wright, and J.M. Scholey. 1992. Immunolocalization of kinesin in sea urchin coelomocytes. Association of kinesin with intracellular organelles. *J. Cell Sci.* 103:309–320.
Herskovits, J.S., C.C. Burgess, R.A. Obar, and R.B. Vallee. 1993*a*. Effects of mutant rat dynamin on endocytosis. *J. Cell Biol.* 122:565–578.
Herskovits, J.S., H.S. Shpetner, C.C. Burgess, and R.B. Vallee. 1993*b*. Microtubules and Src homology 3 domains stimulate the dynamin GTPase via its C-terminal domain. *Proc. Natl. Acad. Sci. USA.* 90:11468–11472.
Hinshaw, J.E., and S.L. Schmid. 1995. Dynamin self-assembles into rings suggesting a mechanism for coated vesicle budding. *Nature (Lond.).* 374:190–192.
Hortsch, M., D. Avossa, and D.I. Meyer. 1986. Characterization of secretory protein translocation: ribosome-membrane interaction in endoplasmic reticulum. *J. Cell Biol.* 103:241–253.
Howell, K.E., and G.E. Palade. 1982. Hepatic Golgi fractions resolved into membrane and content subfractions. *J. Cell Biol.* 92:822–832.
Howell, K.E., R. Schmid, J. Ugelstad, and J. Gruenberg 1989. Immunoisolation using magnetic solid supports: subcellular fractionation for cell-free functional studies. *In* Methods in Cell Biology. A.M. Tartakoff, editor. Academic Press, San Diego, CA. 265–292.
Kelly, R.B. 1995. Ringing necks with dynamin. *Nature (Lond.).* 374:116–117.
Kessell, I., B.D. Holst, and T.F. Roth. 1989. Membranous intermediates in endocytosis are labile, as shown in a temperature-sensitive mutant. *Proc. Natl. Acad. Sci. USA.* 86:4968–4972.
Kim, Y., and C. Wu. 1987. Reversible blockage of neurite development and growth cone formation in neuronal cultures of a temperature-sensitive mutant of *Drosophila. J. Neurosci.* 7:3245–3255.
Koenig, J.H., and K. Ikeda. 1989. Disappearance and reformation of synaptic vesicle membrane upon transmitter release observed under reversible blockage of membrane retrieval. *J. Neurosci.* 9:3844–3860.
Koenig, J.H., and K. Ikeda. 1990. Transformational process of the endosomal compartment in nephrocytes of *Drosophila melanogaster. Cell Tissue Res.* 262:233–244.
Kosaka, T., and K. Ikeda. 1983*a*. Possible temperature-dependent blockage of synaptic vesicle recycling induced by a single gene mutation in *Drosophila. J. Neurobiol.* 14:207–225.
Kosaka, T., and K. Ikeda. 1983*b*. Reversible blockage of membrane retrieval and endocytosis in the garland cell of the temperature-sensitive mutant of *Drosophila melanogaster, shibire*^{ts1}. *J. Cell Biol.* 97:499–507.
Kurzchalia, T.V., P. Dupree, and S. Monier. 1994. VIP21-caveolin, a protein of the trans-Golgi network and caveolae. *FEBS Lett.* 346:88–91.
Laemmli, U.K. 1970. Cleavage of structural proteins during the assembly of the head of bacteriophage T_4. *Nature (Lond.).* 227:680–685.
Larkin, J.M., E.S. Sztul, and G.E. Palade. 1986. Phosphorylation of the rat hepatic polymeric IgA receptor. *Proc. Natl. Acad. Sci. USA.* 83:4759–4763.
Leelavathi, D.E., L.W. Estes, D.S. Feingold, and B. Lombardi. 1970. Isolation of a Golgi-rich fraction from rat liver. *Biochim. Biophys. Acta.* 211:124–138.
Leopold, P.L., A.W. McDowall, K.K. Pfister, G.S. Bloom, and S.T. Brady. 1992. Association of kinesin with characterized membrane-bounded organelles. *Cell Motil. Cytoskeleton.* 23:19–33.
Maeda, K., T. Nakata, Y. Noda, R. Sato-Yoshitake, and N. Hirokawa. 1992. Interaction of dynamin with microtubules: its structure and GTPase activity investigated by using highly purified dynamin. *Mol. Biol. Cell.* 3:1181–1194.
Marks, D.M., J.M. Larkin, and M.A. McNiven. 1994. Association of kinesin with the Golgi apparatus in rat hepatocytes. *J. Cell Sci.* 107:2417–2426.
Montmayeur, J.-P., and E. Borrelli. 1994. Targeting of $G\alpha_{i2}$ to the Golgi by alternative spliced carboxyl-terminal region. *Science (Wash. DC).* 263:95–98.
Moremen, K.W., O. Touster, and P.W. Robbins. 1991. Novel purification of the catalytic domain of Golgi α-mannosidase II: characterization and comparison with the intact enzyme. *J. Biol. Chem.* 266:16876–16885.
Nakata, T., A. Iwamoto, Y. Noda, R. Takemura, H. Yoshikura, and N. Hirokawa. 1991. Predominant and developmentally regulated expression of dynamin in neurons. *Neuron.* 7:461–469.
Nakata, T., R. Takemura, and N. Hirokawa. 1993. A novel member of the dynamin family of GTP-binding proteins is expressed specifically in the testis. *J. Cell Sci.* 105:1–5.
Nangaku, M., R. Sato-Yoshitake, Y. Okada, Y. Noda, R. Takemura, H. Yamazaki, and N. Hirokawa. 1994. KIF1B, a novel microtubule plus end–directed monomeric protein for transport of mitochondria. *Cell.* 79:1209–1220.
Noda, Y., T. Nakata, and N. Hirokawa. 1993. Localization of dynamin: widespread distribution in mature neurons and association with membranous organelles. *Neuroscience.* 55:113–127.
Obar, R.A., C.A. Collins, J.A. Hammarback, H.S. Shpetner, and R.B. Vallee. 1990. Molecular cloning of the microtubule-associated mechanochemical enzyme dynamin reveals homology with a new family of GTP-binding proteins. *Nature (Lond.).* 347:256–261.
Okada, Y., H. Yamazaki, Y. Sekine-Aizawa, and N. Hirokawa. 1995. The neuron-specific kinesin superfamily protein KIF1A is a unique monomeric motor for anterograde axonal transport of synaptic vesicle precursors. *Cell.* 81: 769–780.
Peters, P.J., V.W. Hsu, C.E. Ooi, D. Finazzi, S.B. Teal, V. Oorschot, J.G. Donaldson, and R.D. Klausner. 1995. Overexpression of wild-type and mutant ARF1 and ARF6: distinct perturbations of nonoverlapping membrane compartments. *J. Cell Biol.* 128:1003–1017.
Pfister, K.K., M.C. Wagner, D.L. Stenoien, S.T. Brady, and G.S. Bloom. 1989. Monoclonal antibodies to kinesin heavy and light chains stain vesicle-like structures, but not microtubules, in cultured cells. *J. Cell Biol.* 108:1453–1463.
Pittelkow, M.R., and G.D. Shipley. 1989. Serum-free culture of normal human melanocytes: growth kinetics and growth factor requirements. *J. Cell. Physiol.* 140:565–576.
Poodry, C.A. 1990. *Shibire*, a neurogenic mutant of *Drosophila. Dev. Biol.* 138: 464–472.
Poodry, C.A., and L. Edgar. 1979. Reversible alterations in the neuromuscular junctions of *Drosophila melanogaster* bearing a temperature-sensitive mutation, *shibire. J. Cell Biol.* 81:520–527.
Riezman, H. 1993. Three clathrin-dependent budding steps and cell polarity. *Trends Cell Biol.* 3:330–332.
Robinson, M.S. 1994. The role of clathrin, adaptors and dynamin in endocytosis. *Curr. Opin. Cell Biol.* 6:538–544.
Robinson, P.J., J.-M. Sontag, J.-P. Liu, E.M. Fykse, C. Slaughter, H. McMahon, and T.C. Südhof. 1993. Dynamin GTPase regulated by protein kinase C phosphorylation in nerve terminals. *Nature (Lond.).* 365:163–166.
Robinson, P.J., J.-P. Liu, K.A. Powell, E.M. Fykse, and T.C. Südhof. 1994. Phosphorylation of dynamin 1 and synaptic-vesicle recycling. *Trends Neurosci.* 17:348–353.
Rothman, J.H., C.K. Raymond, T. Gilbert, P.J. O'Hara, and T.H. Stevens. 1990. A putative GTP binding protein homologous to interferon-inducible Mx proteins performs an essential function in yeast protein sorting. *Cell.* 61: 1063–1074.
Scaife, R., and R.L. Margolis. 1990. Biochemical and immunochemical analysis of rat brain dynamin interaction with microtubules and organelles in vivo and in vitro. *J. Cell Biol.* 111:3023–3033.
Scaife, R., I. Gout, M.D. Waterfield, and R.L. Margolis. 1994. Growth-factor–induced binding of dynamin to signal transduction proteins involves sorting to distinct and separate proline-rich dynamin sequences. *EMBO (Eur. Mol. Biol. Org.) J.* 13:2574–2582.
Schmid, S.L. 1992. The mechanism of receptor-mediated endocytosis: more questions than answers. *BioEssays.* 14:589–596.
Schmitz, F., K.T. Wallis, M. Rho, D. Drenckhahn, and D.B. Murphy. 1994. Intracellular distribution of kinesin in chromaffin cells. *Eur. J. Cell Biol.* 63:77–83.
Shpetner, H.S., and R.B. Vallee. 1989. Identification of dynamin, a novel mechanochemical enzyme that mediates interactions between microtubules. *Cell.* 59:421–432.
Shpetner, H.S., and R.B. Vallee. 1992. Dynamin is a GTPase stimulated to high levels of activity by microtubules. *Nature (Lond.).* 355:733–735.
Smart, E.J., Y.S. Ying, P.A. Conrad, and R.G. Anderson. 1994. Caveolin moves from caveolae to the Golgi apparatus in response to cholesterol oxidation. *J. Cell Biol.* 127:1185–1197.
Sontag, J.-M., E.M. Fykse, Y. Ushkaryov, J.-P. Liu, P.J. Robinson, and T.C. Südhof. 1994. Differential expression and regulation of multiple dynamins. *J. Biol. Chem.* 269:4547–4554.
Sztul, E.S., K.E. Howell, and G.E. Palade. 1985. Biogenesis of the polymeric IgA receptor in rat hepatocytes. II. Localization of its intracellular forms by cell fractionation studies. *J. Cell Biol.* 100:1255–1261.
Takei, K., P.S. McPherson, S.L. Schmid, and P. De Camilli. 1995. Tubular membrane invaginations coated by dynamin rings are induced by GTP-γS in nerve terminals. *Nature (Lond.).* 374:186–190.
Towbin, H., T. Staehelin, and J. Gordon. 1979. Electrophoretic transfer of proteins from polyacrylamide gels to nitrocellulose sheets: procedure and some applications. *Proc. Natl. Acad. Sci. USA.* 76:4350–4354.
Tuma, P.L., M.C. Stachniack, and C.A. Collins. 1993. Activation of dynamin GTPase by acidic phospholipids and endogenous rat brain vesicles. *J. Biol. Chem.* 268:17240–17246.

van der Bliek, A.M., and E.M. Meyerowitz. 1991. Dynamin-like protein encoded by the *Drosophila shibire* gene associated with vesicular traffic. *Nature (Lond.).* 351:411–414.

van der Bliek, A.M., T.E. Redelmeier, H. Damke, E.J. Tisdale, E.M. Meyerowitz, and S.L. Schmid. 1993. Mutations in human dynamin block an intermediate stage in coated vesicle formation. *J. Cell Biol.* 122:553–563.

Vater, C.A., C.K. Raymond, K. Ekena, I. Howald-Stevenson, and T.H. Stevens. 1992. The *VPS1* protein, a homolog of dynamin required for vacuolar protein sorting in *Saccharomyces cerevisiae*, is a GTPase with two functionally separable domains. *J. Cell Biol.* 119:773–786.

Welsh, C.F., J. Moss, and M. Vaughan. 1994. ADP-ribosylation factors: a family of approximately 20-kDa guanine nucleotide-binding proteins that activate cholera toxin. *Mol. Cell. Biochem.* 138:157–166.

Wilsbach, K., and G.S. Payne. 1993. Vps1p, a member of the dynamin GTPase family, is necessary for Golgi membrane protein retention in *Saccharomyces cerevisiae*. *EMBO (Eur. Mol. Biol. Org.) J.* 12:3049–3059.

Wood, S.A., J.E. Park, and W.J. Brown. 1991. Brefeldin A causes a microtubule-mediated fusion of the Golgi network and early endosomes. *Cell.* 67: 591–600.